Korean J. Chem. Eng., 33(2), 683-687 (2016)
DOI: 10.1007/s11814-015-0144-5

pISSN: 0256-1115
eISSN: 1975-7220

Synthesis of rare earth oxide nanoplates with single unit cell thickness using a thermal decomposition method

Euiyoung Jung, Taekyung Yu, and Woo-Sik Kim†

Department of Chemical Engineering, Kyung Hee University, Yongin 446-701, Korea
(*Received 16 April 2015 • accepted 29 June 2015*)

Abstract−We report the colloidal synthesis of rare earth oxide nanoplates with square and disk shapes using thermal decomposition of $Ln(CH_3CO_2)_3 \cdot xH_2O$ in the presence of a mixture of oleylamine and oleic acid (Ln=La, Pr, Nd, Dy, Er, and Y). In this synthesis, oleylamine plays an important role in the formation of ultra-thin nanoplates with thickness of 1.1 nm, which corresponds to a single unit cell dimension of rare earth oxides, and oleic acid serves as a capping agent for the formation of nanoplates having nano-sized side dimension (around 15-40 nm). By varying the rare earth precursors, we obtained square-shaped nanoplates (La_2O_3, Pr_2O_3, and Nd_2O_3) and disk-shaped nanoplates (Dy_2O_3, Er_2O_3, and Y_2O_3), respectively, confirming that our synthesis could be extended to the synthesis of various rare earth oxide nanoplates.

Keywords: Rare Earth Oxide, Nanoplates, Single Unit Cell Thickness, Thermal Decomposition, Oleylamine, Oleic Acid

INTRODUCTION

Rare earth oxide nanocrystals with controllable sizes and shapes have received intense research attention during the past few years due to their potential applications in optics [1-3], optoelectronics, biological labeling [4-7], and catalysis [8]. There have been various chemical methods for synthesis of rare earth oxide nanocrystals including hydrothermal, precipitation, non-hydrolytic sol-gel, and thermal decomposition method [9-32]. Among the various shaped rare earth oxide nanocrystals, ultra-thin nanoplates with thickness of less than 1.1 nm are of particular interest because they are formed by assembly of single layer of unit cells, and thus have high surface-to-volume ratio compared with nanocrystals having different morphologies [32]. Cao reported the synthesis of square-shaped gadolinium oxide (Gd_2O_3) nanoplates with a thickness of 1.1 nm [14]. Hyeon and co-workers were also able to design the thermal decomposition route for synthesis of uniform samarium oxide (Sm_2O_3) nanowires and nanoplates with a single unit cell thickness [19]. However, a facile synthetic method that is applicable to of the general rare earth oxide nanoplates has not been reported yet. Recently, Yan and co-workers reported the synthesis of various rare earth oxide nanocrsytals including ultra-thin nanoplates, but the synthetic procedure required multiple and tedious steps to prepare precursor complexes, for example, metal-1-benzoylacetone complex [16]. Herein, we report on a facile synthesis of rare earth oxide nanoplates including lanthanum oxide (La_2O_3), praseodymium oxide (Pr_2O_3), neodymium oxide (Nd_2O_3), dysoprosium oxide (Dy_2O_3), erbium oxide (Er_2O_3), and yttrium oxide (Y_2O_3) with a single unit cell thickness using thermal decomposition of rare earth acetate as a precursor in the presence of a mixture of oleylamine and oleic acid. We found that oleylamine and oleic acid play key roles in the formation of ultra-thin nanoplates with nano-sized side dimension (around 15-20 nm). In this synthesis, we can obtain ultra-thin rare earth oxide nanoplates with high quality, just by heating three components - rare earth acetate, oleic acid, and oleylamine - showing that this synthetic method is a simple and versatile method for synthesis of other metal oxide nanoparticles.

EXPERIMENTAL SECTION

1. Materials

Lanthanum(III) acetate hydrate ($La(CH_3CO_2)_3 \cdot xH_2O$), Lanthanum(III) chloride ($LaCl_3$), praseodymium(III) acetate hydrate ($Pr(CH_3CO_2)_3 \cdot xH_2O$), neodymium(III) acetate hydrate ($Nd(CH_3CO_2)_3 \cdot xH_2O$), dysoprosium(III) acetate hydrate ($Dy(CH_3CO_2)_3 \cdot xH_2O$), erbium(III) acetate hydrate ($Er(CH_3CO_2)_3 \cdot xH_2O$), yttrium acetate hydrate ($Y(CH_3CO_2)_3 \cdot xH_2O$), oleic acid (99%), and oleylamine were purchased from Aldrich and used without further purification.

2. Synthesis of Rare Earth Oxide Nanoplates

In a typical synthesis, 2 mmol of $Ln(CH_3CO_2)_3 \cdot xH_2O$ (Ln=La, Pr, Nd, Dy, Er, and Y) was added to a mixture solvent composed of 60 mmol of oleylamine and 18 mmol of oleic acid at room temperature. The resulting solution was heated to 90 °C in a vacuum to remove hydrated water, forming a homogeneous and clear white-yellow solution. The resulting mixture was then heated to 320 °C and aged at that temperature for 2 h in argon (Ar) atmosphere. After the reaction was finished, 100 mL of ethanol was added to induce the precipitation of the nanoplates. The precipitate was retrieved by centrifugation, and the resulting nanoplates were dispersible in many organic solvents, such as toluene, hexane, and octane.

3. Characterization

TEM and high-resolution TEM (HRTEM) images were captured

†To whom correspondence should be addressed.
E-mail: wskim@khu.ac.kr
‡This article is dedicated to Prof. Hwayong Kim on the occasion of his retirement from Seoul National University.

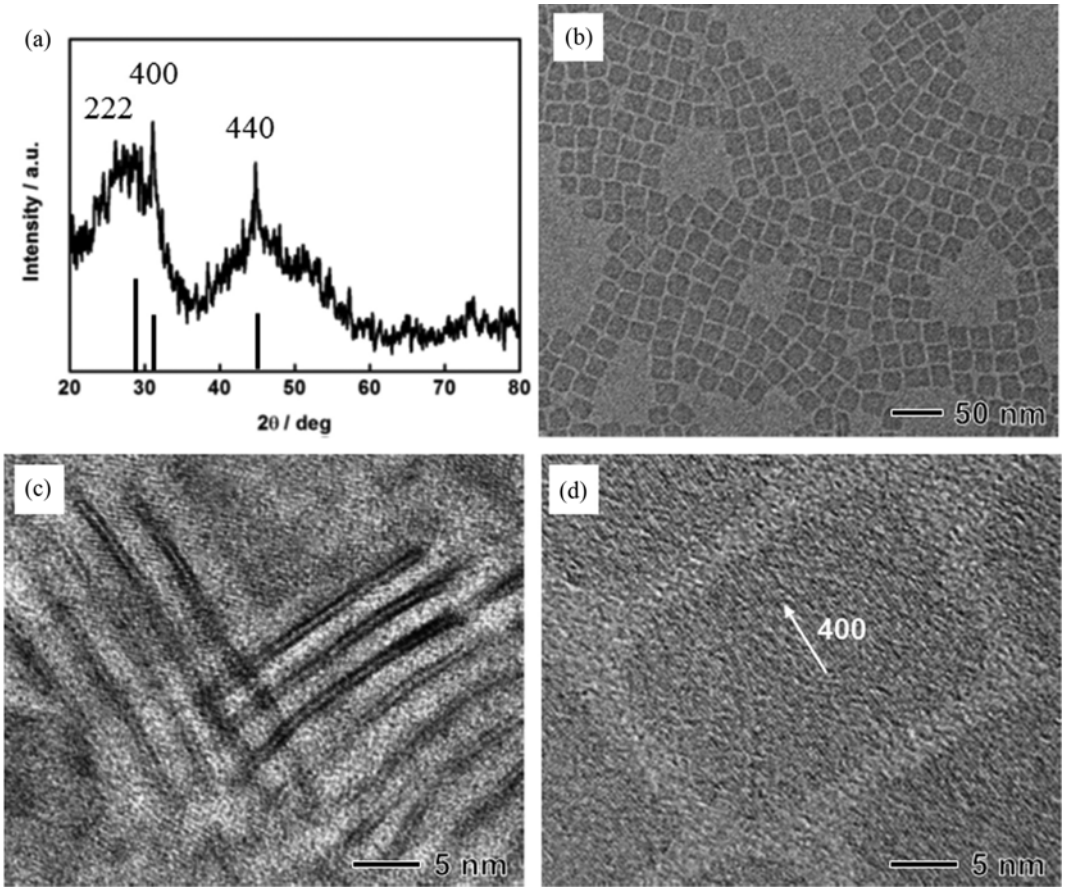

Fig. 1. (a) Powder XRD pattern, (b) TEM image, and (c), (d) HRTEM images of square-shaped La_2O_3 nanoplates synthesized by thermal decomposition of $La(CH_3CO_2)_3 \cdot xH_2O$ in the presence of a mixture of oleylamine and oleic acid at 320 °C for 2 h.

by using a JEM-2100F microscope operated at 200 kV. The powder X-ray diffraction (XRD) patterns were obtained with a Rigaku D-MAX/A diffractometer at 35 kV and 35 mA.

RESULTS AND DISCUSSION

Ln_2O_3 nanoplates were synthesized by thermal decomposition of $Ln(CH_3CO_2)_3 \cdot xH_2O$ in the presence of a mixture of oleylamine and oleic acid. The powder X-ray diffraction (XRD) patterns (Fig. 1(a)) taken from the as-synthesized La_2O_3 nanoplates show strong peaks at 27° (222), 32° (400), and 45° (440), respectively, which are matched well with the standard pattern of bcc La_2O_3 (*La3*, a=11.32 Å, Joint Committee on Powder Diffraction Standards (JCPDS) file number 22-0369). Note that there are two crystal phases in La_2O_3, cubic and hexagonal (JCPDS file number 83-1355) phase. In the XRD patterns, small peaks at 26° and 52° are also found, suggesting the existence of small fraction of hexagonal La_2O_3 phase. However, because the strongest (101) peak of hexagonal La_2O_3 phase at 28.9° is missing in the XRD patterns of the nanoplates, we can claim that bcc La_2O_3 phase is dominant in the product. A transmission electron microscopic (TEM) image of La_2O_3 nanoplates shows that the nanoplates have side dimensions of around 15 nm (Fig. 1(b)). A high-resolution TEM (HRTEM) image of nanoplates standing perpendicular on the substrate reveals that the thickness of nanoplates is around 1.1 nm, which correspond to the size of one unit cell (Fig. 1(c)). Also, an HRTEM image of faceted nanoplates resting on its face shows that the edges of the square-shape nanoplate are surrounded by (100) planes (Fig. 1(d)).

Recently, many anisotropic nanocrystals, including nanorods, nanoplates, and nanowires, have been synthesized by introducing two different kinds of capping agents having different binding capabilities. In the present synthesis, oleic acid and oleylamine were used as both capping agent and reacting solvent. Oleic acid tends to attach on the surface of oxide nanocrystals more strongly than oleylamine, due to its higher oxophilicity. To understand the role of oleic acid and oleylamine, we performed control experiments in absence of oleic acid or oleylamine, while keeping other reaction conditions the same as those in the synthesis of La_2O_3 nanoplates shown in Fig. 1. In the synthesis of Mn_3O_4 nanocrystals with various shapes, Hyeon and co-workers proposed that selective attachment of oleylamine onto the (001) facet of Mn_3O_4 nanocrystals led to the formation of plate shaped nanocrystals [33]. When the synthesis was conducted using only oleylamine as both capping agent and solvent, large plates with side dimension of around 400 nm were observed (Fig. 2(a)). On the other hand, we could not find the formation of any nanocrystals in the resulting solution when only oleic acid was used as the solvent. We think that this can be attributed to the formation of La-oleate complex due to the strong binding of

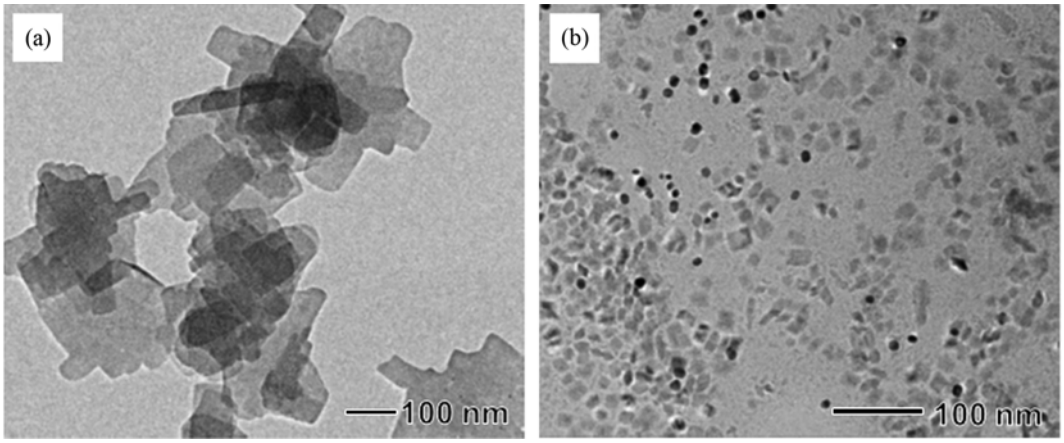

Fig. 2. (a) TEM image of a sample prepared under the same conditions as those in Fig. 1 except that the synthesis was conducted in the absence of oleic acid. (b) TEM image of a sample prepared under the same conditions as those in Fig. 1 except that the synthesis was conducted in the presence of $LaCl_3$ instead of $La(CH_3CO_2)_3 \cdot xH_2O$.

oleic acid to La^{3+} ion [19]. These results demonstrate that oleylamine plays an important role in the formation of ultra-thin nanoplates, whereas oleic acid serves as a co-surfactant for formation of nanoplates having nano-sized side dimension. In addition, when we used $LaCl_3$ instead of $La(CH_3CO_2)_3 \cdot xH_2O$ as a precursor, irregular shaped La_2O_3 nanoplates were synthesized, indicating that activity of precursor is also important to the formation of uniform nanoplates (Fig. 2(b)).

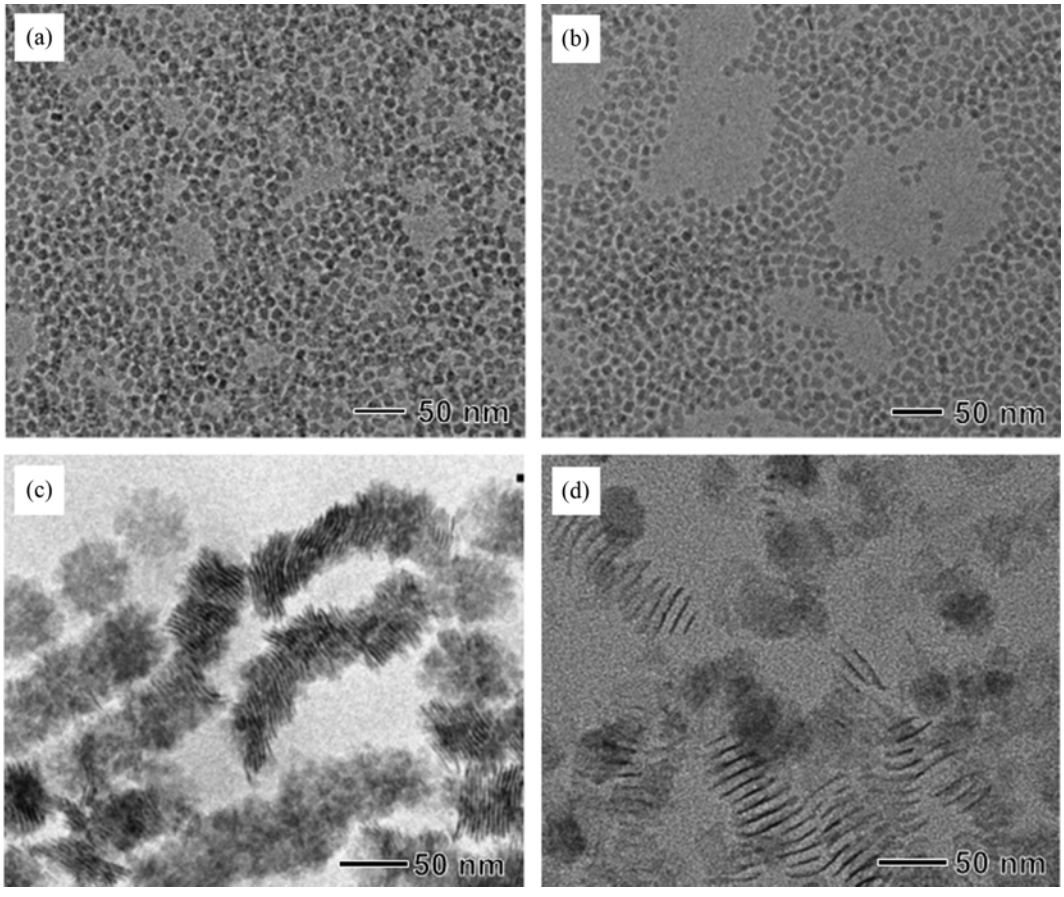

Fig. 3. TEM images of square-shaped (a) Pr_2O_3 and (b) Nd_2O_3 nanoplates prepared under the same conditions as those in Fig. 1 except that the synthesis was conducted in the presence of $Pr(CH_3CO_2)_3 \cdot xH_2O$ and $Nd(CH_3CO_2)_3 \cdot xH_2O$ as a precursor, respectively, and (c) Dy_2O_3 and (b) Er_2O_3 nanoplates with disk shape prepared under the same conditions as those in Fig. 1 except that the synthesis was conducted in the presence of $Dy(CH_3CO_2)_3 \cdot xH_2O$ and $Er(CH_3CO_2)_3 \cdot xH_2O$ as a precursor, respectively.

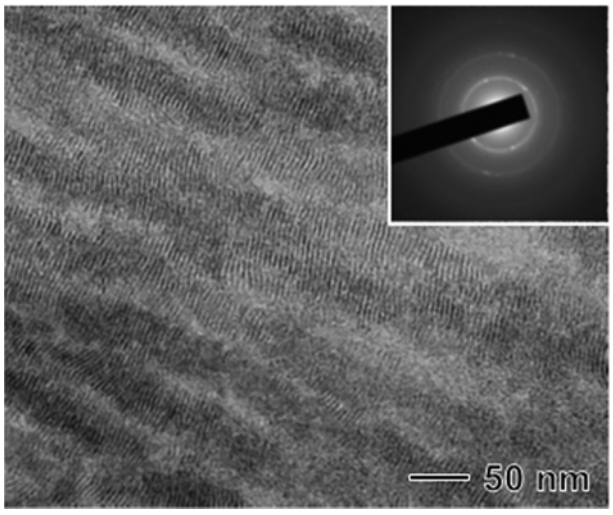

Fig. 4. TEM image of Y_2O_3 nanoplates prepared under the same conditions as those in Fig. 1 except that the synthesis was conducted in the presence of $Y(CH_3CO_2)_3 \cdot xH_2O$ as a precursor.

Rare earth elements, a set of seventeen chemical elements which include the fifteen lanthanides as well as scandium and yttrium, have similar chemical and physical properties. Therefore, we thought that our synthesis could be extended to the other rare earth oxides including Pr, Nd, Dy, Er, and Y. When we used $Pr(CH_3CO_2)_3 \cdot xH_2O$ and $Nd(CH_3CO_2)_3 \cdot xH_2O$ as a precursor while keeping the other experimental conditions unchanged, square-shaped Pr_2O_3 and Nd_2O_3 nanoplates with side dimensions of around 10 nm were synthesized, respectively (Fig. 3(a) and (b)). By changing precursor to $Dy(CH_3CO_2)_3 \cdot xH_2O$ and $Er(CH_3CO_2)_3 \cdot xH_2O$, the morphology of the nanoplates was varied from square-plate to disk-shaped nanoplates (Dy_2O_3 and Er_2O_3) with larger sizes of around 40 nm, demonstrating that activity of lanthanide precursor would be critical for the size and morphology of nanoplates (Fig. 3(c) and (d)). Interestingly, TEM images of all nanoplates exhibit ultra-thin thickness of around 1.1 nm, which correspond to a single unit cell dimension of rare earth oxides. In addition, we could also synthesize Y_2O_3 nanoplates using the same procedure as that employed for the synthesis of the La_2O_3 nanoplates (Fig. 4). Recently, Eu-doped Y_2O_3 nanoplates have been prepared in the same manner and we are trying to use them to increase the photocurrent of a dye-sensitized solar cell (DSSC).

CONCLUSIONS

We synthesized rare earth oxide nanoplates, including La_2O_3, Pr_2O_3, Nd_2O_3, Dy_2O_3, Er_2O_3, and Y_2O_3, by using thermal decomposition of $Ln(CH_3CO_2)_3 \cdot xH_2O$ in the presence of a mixture of oleylamine and oleic acid. The synthesized nanoplates exhibit an ultra-thin thickness of around 1.1 nm, corresponding to a single unit cell dimension. By varying the experimental conditions, we find that oleylamine plays an important role in the formation of ultra-thin nanoplates and oleic acid serves as a capping agent for formation of nanoplates having nano-sized side dimension. In this synthesis, we can obtain ultra-thin rare earth oxide nanoplates with high quality, just by heating three components - rare earth acetate, oleic acid, and oleylamine - showing that this synthetic method is simple and versatile for synthesis of other metal oxide nanoparticles.

ACKNOWLEDGEMENT

This work was financially supported by the Kyung Hee University Research Program (2013).

REFERENCES

1. K. Riwotzki, H. Meyssamy, H. Schnablegger, A. Kornowski and M. Haase, *Angew. Chem. Int. Ed.*, **40**, 573 (2001).
2. J. W. Stouwdam and F. C. van Weggel, *Nano Lett.*, **2**, 733 (2002).
3. S. Heer, O. Lehmann, M. Haase and H. U. Gudel, *Angew. Chem. Int. Ed.*, **42**, 3179 (2003).
4. G. S. Yi, H. C. Lu, S. Y. Zhao, G. Yue, W. J. Yang, D. P. Chen and L. H. Guo, *Nano Lett.*, **4**, 2191 (2004).
5. L. Y. Wang, R. X. Yan, Z. Y. Huo, L. Wang, J. H. Zeng, J. Bao, H. K. Wu, X. Wang, Q. Peng and Y. D. Li, *Angew. Chem. Int. Ed.*, **44**, 6054 (2005).
6. J. H. Zeng, J. Su, Z. H. Li, R. X. Yan and Y. D. Li, *Adv. Mater.*, **17**, 2119 (2005).
7. R. X. Yan and Y. D. Li, *Adv. Funct. Mater.*, **15**, 763 (2005).
8. K. B. Zhou, X. Wang, X. M. Sun, Q. Peng and Y. D. Li, *J. Catal.*, **229**, 206 (2005).
9. Y. Xie, Y. Qian, W. Wang, S. Zhang and Y. Zhang, *Science*, **272**, 1926 (1996).
10. J. Zhang, X. Ju, Z. Y. Wu, T. Liu, T. D. Hu, Y. N. Xie and Z. L. Zhang, *Chem. Mater.*, **13**, 4192 (2001).
11. X. Wang and Y. D. Li, *Angew. Chem. Int. Ed.*, **41**, 4790 (2002).
12. M. Yada, M. Mihara, S. Mouri, M. Kuroki and T. Kijima, *Adv. Mater.*, **14**, 309 (2002).
13. M. Yamashita, K. Kameyama, S. Yabe, S. Yoshida, Y. Fujishiro, T. Kawai and T. Sato, *J. Mater. Sci.*, **37**, 683 (2002).
14. Y. C. Cao, *J. Am. Chem. Soc.*, **126**, 7456 (2004).
15. T. Yu, J. Joo, Y. I. Park and T. Hyeon, *Angew. Chem. Int. Ed.*, **44**, 7411 (2005).
16. R. Si, Y. W. Zhang, L. P. You and C. H. Yan, *Angew. Chem. Int. Ed.*, **44**, 3256 (2005).
17. M. Niederberger and G. Garnweitner, *Chem. Eur. J.*, **12**, 7282 (2006).
18. G. Zou, H. Li, Y. G. Zhang, K. Xiong and Y. Qian, *Nanotech.*, **17**, S313 (2006).
19. T. Yu, J. Joo, Y. I. Park and T. Hyeon, *J. Am. Chem. Soc.*, **128**, 1786 (2006).
20. J. Park, J. Joo, S. G. Kwon, Y. Jang and T. Hyeon, *Angew. Chem. Int. Ed.*, **46**, 4630 (2007).
21. R. Si, Y. Zhang, H. Zhou, L. Sun and C. Yan, *Chem. Mater.*, **19**, 18 (2007).
22. J. Zhang, S. Ohara, M. Umetsu, T. Naka, Y. Hatakeyama and T. Adschiri, *Adv. Mater.*, **19**, 203 (2007).
23. Z. Huo, C. Tsung, W. Huang, M. Fardy, R. Yan, X. Zhang, Y. Li and P. Yang, *Nano Lett.*, **9**, 1260 (2009).
24. K. Kattel, J. Y. Park, W. Xu, H. G. Kim, E. J. Lee, B. A. Bony, W. C. Heo, J. J. Lee, S. Jin, J. S. Baeck, Y. Chang, T. J. Kim, J. E. Bae, K. S. Chae and G. H. Lee, *ACS Appl. Mater. Interfaces*, **3**, 3325 (2011).
25. S. S. Lee, H. Zhu, E. Q. Contreras, A. Prakash, H. L. Puppala and

V. L. Colvin, *Chem. Mater.*, **24**, 424 (2011).
26. D. Wang, Y. Kang, V. Doan-Nguyen, J. Chen, R. Kungas, N. L. Wieder, K. Bakhmutsky, R. J. Gorte and C. B. Murray, *Angew. Chem. Int. Ed.*, **50**, 4378 (2011).
27. G. Lee, Y.-S. Cho, S. Park and G.-R. Yi, *Korean J. Chem. Eng.*, **28**, 1641 (2011).
28. K. Kattel, J. Y. Park, W. Xu, H. G. Kim, E. J. Lee, B. A. Bony, W. C. Heo, S. Jin, J. S. Baeck, Y. Chang, T. J. Kim, J. E. Bae, K. S. Chae and G. H. Lee, *Biomaterials*, **33**, 3254 (2012).
29. M. Kim, H.-S. Lee, Y. H. Shin, K. H. Ahn, Y.-S. Youn, J. Kim and Y.-W. Lee, *Korean J. Chem. Eng.*, **29**, 1289 (2012).
30. T. Paik, T. R. Gordon, A. M. Prantner, H. Yun and C. B. Murray, *ACS Nano*, **7**, 2850 (2013).
31. M. Cho, R. Sethi, J. S. A. narayanan, S. S. Lee, D. N. Benoit, N. Taheri, P. Decuzzi and V. L. Colvin, *Nanoscale*, **6**, 13637 (2014).
32. D. Wang, Y. Kang, X. Ye and C. B. Murray, *Chem. Mater.*, **26**, 6328 (2014).
33. T. Yu, J. Moon, J. Park, Y. I. Park, H. B. Na, B. H. Kim, I. C. Song, W. K. Moon and T. Hyeon, *Chem. Mater.*, **21**, 2272 (2009).